ÓPTICA PURA Y APLICADA
www.sedoptica.es

Type: RIAO OPTILAS 2023
Section: IMAGING TECHNIQUES

PHOTODYNAMIC THERAPY WITH NON-PORPHYRIN PHOTOSENSITIZERS IN BREAST CANCER AND NON-CANCER CELLS

TERAPIA FOTODINÁMICA CON FOTOSENSIBILIZADORES NO PORFIRINOS EN CÉLULAS DE MAMA CANCERÍGENAS Y NO CANCERÍGENAS

JUAN CARLOS ATENCO-CUAUTLE[1a], NAYELI PEREZ-PEREZ[1a], MARIA GUADALUPE DELGADO-LOPEZ[2], JULIAN RAMIREZ-RAMIREZ[1], JULIO CESAR RAMIREZ-SAN-JUAN[1], RUBEN RAMOS-GARCIA[1], TERESITA SPEZZIA-MAZZOCCO[1]*

[a] *Both authors contributed equally*

1.Department of Optics. National Institute of Astrophysics, Optics and Electronics. Luis Enrique Erro No.1, CP 72840, Puebla, México

2.Biomedical Research Center of the East. Mexican Institute of Social Security, Km 4.5 Carretera Atlixco-Metepec, CP 74360, Puebla, México. Affiliation

*terespezzia@inaoe.mx S: miembro de SEDOPTICA / SEDOPTICA member

Received: 04/09/2023 Accepted: 15/01/2024
DOI: 10.7149/OPA.57.1.51161

ABSTRACT:

Breast cancer is a major cause of morbidity and mortality in women worldwide. Conventional therapies have undesirable side effects and in some cases are ineffective; therefore, the search for alternative therapies, such as photodynamic therapy (PDT), is essential. In this work, the effect of PDT on two breast cancer cell lines and one non-cancerous breast cell line was investigated using non-porphyrin photosensitizers (PS), such as methylene blue (MB) and rose bengal (RB). The efficacy of each treatment was evaluated by measuring cell viability with the MTT assay and by morphological observations. Before evaluating the effects of PDT, the intracellular uptake of each PS was measured in the cell lines studied. The results showed that the MDA-MB-231 cell line exhibited the highest sensitivity to PDT for both PS. The T47D cell line showed almost 50% inhibition in both cases. Surprisingly, the non-cancerous cell line MCF10A showed a selective response to PDT. In particular, no significant inhibition was observed with MB-PDT treatment. However, inhibition was observed with RB-PDT treatment. The morphological changes supported the cytopathic effect induced by PDT, it was found that non-cancerous MCF10A cells showed remarkable changes only with the highest dose of RB-PDT. In conclusion, this study presents, to the best of our knowledge, for the first time the effect of PDT using RB as a PS for the inhibition of MDA-MB-231, T47D and MCF10A breast cells, and using MB for PDT inhibition onT47D cells. Furthermore, no direct relationship was observed between the effect of PDT and the intracellular concentration of PS. Finally, these findings highlight the potential of MB and RB as effective PS in PDT and suggest the importance of considering cell line-specific responses and characteristics in optimizing PDT efficacy and selectivity.

Key words: breast cancer, photodynamic therapy, non-porphyrin photosensitizers.

RESUMEN:

El cáncer de mama es una de las principales patologías que causan altas tasas de morbilidad y mortalidad en las mujeres a nivel mundial. Las terapias convencionales tienen efectos secundarios indeseables y en algunos casos, son ineficaces; por ello, la búsqueda de terapias alternativas, como la terapia fotodinámica (TFD), es fundamental. En este trabajo se investigó el efecto de la TFD sobre dos líneas celulares de cáncer de mama y una línea celular de mama no cancerígena, utilizando fotosensibilizadores (FS) no porfirínicos, como el azul de metileno (AM) y el rosa de bengala (RB). La

eficacia de cada tratamiento se evaluó midiendo la viabilidad celular con el ensayo MTT y mediante observaciones morfológicas. Antes de evaluar los efectos de la TFD, se midió la absorción intracelular de cada FS en las líneas celulares estudiadas. Los resultados obtenidos mostraron que la línea celular MDA-MB-231, presentó la mayor sensibilidad a la PDT para ambos tratamientos de TFD. La línea celular T47D presentó casi un 50% de inhibición en ambos casos. Sorprendentemente, la línea celular MCF10A, no cancerígena, mostró una respuesta selectiva a la TFD. En particular, no se observó una inhibición importante empleando el tratamiento con MB-PDT. Sin embargo, si se observó inhibición con el tratamiento de RB-PDT. Los cambios morfológicos respaldaron el efecto citopático inducido por la TFD, donde fue evidente que las células MCF10A no cancerosas mostraron cambios notables solo con la dosis más alta de RB-PDT. En conclusión, este estudio presenta por primera vez el efecto de la TFD utilizando RB como fotosensibilizador para la inhibición de las células mamarias MDA-MB-231, T47D y MCF10A, y usando MB-PDT para la inhibición de las células T47D. Por último, no se observó una relación directa entre el efecto de la TFD y la concentración intracelular del FS.

Palabras clave: cáncer de mama, terapia fotodinámica, fotosensibilizadores no porfirínicos.

REFERENCES

[1] B. Timmermans, A. De Las Peñas, I. Castaño, and P. Van Dijck, "Adhesins in Candida glabrata," J. Fungi, **4**, 60 (2018).

[2] X. Zhao, H. Ma, J. Chen, F. Zhang, X. Jia, and J. Xue, "An epidermal growth factor receptor-targeted and endoplasmic reticulum-localized organic photosensitizer toward photodynamic anticancer therapy," Eur. J. Med. Chem., **182**, 111625 (2019).

[3] N. N. Peskova et al., "The localization of the photosensitizer determines the dynamics of the secondary production of hydrogen peroxide in cell cytoplasm and mitochondria," J. Photochem. Photobiol. B Biol., **219**, 112208 (2021).

[4] A. Burguin, C. Diorio, and F. Durocher, "Breast Cancer Treatments: Updates and New Challenges," *J.* Pers. Med., **11**, 808 (2021).

[5] H. Burioka, U. Yamamori, N. Nagano, A. Ue, and Y. Tamaki, "Radiation Therapy for Breast Cancer With Oligometastatic Cervical Lymph Nodes: A Case Report," Cureus (2024).

[6] F. Ye *et al.*, "Advancements in clinical aspects of targeted therapy and immunotherapy in breast cancer," Mol. Cancer, **22**, 105 (2023).

[7] L. A. Emens and S. Loi, "Immunotherapy Approaches for Breast Cancer Patients in 2023," Cold Spring Harb. Perspect. Med., **13**, a041332 (2023).

[8] C. S. Oliveira, R. Turchiello, A. J. Kowaltowski, G. L. Indig, and M. S. Baptista, "Major determinants of photoinduced cell death: Subcellular localization versus photosensitization efficiency," Free Radic. Biol. Med., **51**, 824–833 (2011).

[9] D. Kessel and J. J. Reiners, "Enhanced Efficacy of Photodynamic Therapy via a Sequential Targeting Protocol," Photochem. Photobiol., **90**, 889-95 (2014).

[10] R. A. Leon-Ferre and M. P. Goetz, "Advances in systemic therapies for triple negative breast cancer," BMJ, e071674 (2023).

[11] A. P. Castano, T. N. Demidova, and M. R. Hamblin, "Mechanisms in photodynamic therapy: part one—photosensitizers, photochemistry and cellular localization," Photodiagnosis Photodyn. Ther., **1**, 279–293 (2004).

[12] R. R. Allison and C. H. Sibata, "Oncologic photodynamic therapy photosensitizers: A clinical review," Photodiagnosis Photodyn. Ther., **7,** 61–75 (2010).

[13] J. P. Tardivo et al., "Methylene blue in photodynamic therapy: From basic mechanisms to clinical applications," Photodiagnosis Photodyn. Ther., **2**, 175–191 (2005).

[14] N. Vanerio, M. Stijnen, B. A. J. M. de Mol, and L. M. Kock, "Biomedical Applications of Photo- and Sono-Activated Rose Bengal: A Review," Photobiomodulation, Photomedicine, Laser Surg., **37,** 383–394 (2019).

[15] M. F. Loya-Castro et al., "Preparation of PLGA/Rose Bengal colloidal particles by double emulsion and layer-by-layer for breast cancer treatment," J. Colloid Interface Sci., **518**, 122–129 (2018).

[16] A. Douplik, G. Saiko, I. Schelkanova, and V. V. Tuchin, "The response of tissue to laser light," in Lasers for Medical Applications, Elsevier, , 47–109 (2013).

[17] C. Puyana, R. Bunney, E. C. N. Kaminska, S. Pei, and M. M. Tsoukas, "Photodynamic Therapy for Malignant Skin Lesions," *European Handbook of Dermatological Treatments*. Springer International Publishing, 1403–1421 (2023).

[18] G. Gunaydin, M. E. Gedik, and S. Ayan, "Photodynamic Therapy for the Treatment and Diagnosis of Cancer–A Review of the Current Clinical Status," Front. Chem., **9** (2021).

[19] J. Zou *et al.*, "Evaluation of lensed fibers used in photodynamic therapy (PDT)," Photodiagnosis Photodyn. Ther., **31**, 101924, (2020).

[20] J. F. Algorri, M. Ochoa, P. Roldán-Varona, L. Rodríguez-Cobo, and J. M. López-Higuera, "Light Technology for Efficient and Effective Photodynamic Therapy: A Critical Review," *Cancers (Basel).*, vol. **13**, 3484 (2021).

[21] R. R. Allison and K. Moghissi, "Photodynamic Therapy (PDT): PDT Mechanisms," Clin. Endosc., **46**, 24 (2013).

[22] M. A. Weston and M. S. Patterson, "Monitoring oxygen concentration during photodynamic therapy using prompt photosensitizer fluorescence," Phys. Med. Biol., **58,** 7039–7059 (2013).

[23] A. Borodziuk et al., "Unmodified Rose Bengal photosensitizer conjugated with NaYF 4 :Yb,Er upconverting nanoparticles for efficient photodynamic therapy," Nanotechnology, **31**, 465101, (2020).

[24] A. Torres-Martínez et al., "Non-Polymeric Nanogels as Versatile Nanocarriers: Intracellular Transport of the Photosensitizers Rose Bengal and Hypericin for Photodynamic Therapy," ACS Appl. Bio Mater., **4,** 3658–3669 (2021).

[25] R. Bhole, C. Bonde, P. Kadam, R. Wavwale "A Comprehensive Review on Photodynamic Therapy (PDT) and Photothermal Therapy (PTT) for Cancer Treatment," Turk J Oncol **36,** 125–32 (2021).

[26] A. B. Ormond and H. S. Freeman, "Dye sensitizers for photodynamic therapy," Materials, **6**, 817-840 (2013).

[27] R. W. Redmond and I. E. Kochevar, "Medical Applications of Rose Bengal- and Riboflavin-Photosensitized Protein Crosslinking," Photochem. Photobiol., **95**, 1097–1115 (2019).

[28] D. C. Neckers, "Rose Bengal," J. Photochem. Photobiol. A Chem., **47**, 1–29 (1989).

[29] T. Cwalinski et al., "Methylene Blue—Current Knowledge, Fluorescent Properties, and Its Future Use," J. Clin. Med., **9**, 3538 (2020).

[30] P. Ferenc, P. Solár, J. Kleban, J. Mikeš, and P. Fedoročko, "Down-regulation of Bcl-2 and Akt induced by combination of photoactivated hypericin and genistein in human breast cancer cells," J. Photochem. Photobiol. B Biol., **98**, 25–34 (2010).

[31] R. Montazerabadi, A. Sazgarnia, M. H. Bahreyni-Toosi, A. Ahmadi, and A. Aledavood, "The effects of combined treatment with ionizing radiation and indocyanine green-mediated photodynamic therapy on breast cancer cells," J. Photochem. Photobiol. B Biol., **109**, 42–49 (2012).

[32] A. F. Santos et al., "Fluence Rate Determines PDT Efficiency in Breast Cancer Cells Displaying Different GSH Levels," Photochem. Photobiol., **96**, 658–667 (2020).

[33] S. H. Mousavi, J. Tavakkol-Afshari, A. Brook, and I. Jafari-Anarkooli, "Direct toxicity of Rose Bengal in MCF-7 cell line: Role of apoptosis," Food Chem. Toxicol., **47**, 855–859 (2009).

[34] J. D. Monroe, E. Belekov, A. O. Er, and M. E. Smith, "Anticancer Photodynamic Therapy Properties of Sulfur-Doped Graphene Quantum Dot and Methylene Blue Preparations in MCF7 Breast Cancer Cell Culture," Photochem. Photobiol., **95**, 1473–1481 (2019).

[35] T. A. Theodossiou et al., "Simultaneous defeat of MCF7 and MDA-MB-231 resistances by a hypericin PDT–tamoxifen hybrid therapy," npj Breast Cancer, **5**, 13 (2019).

[36] A. F. dos Santos et al., "Methylene blue photodynamic therapy induces selective and massive cell death in human breast cancer cells," BMC Cancer, **17**, 194 (2017).

[37] R. Hosseinzadeh, K. Khorsandi, and M. Jahanshiri, "Combination photodynamic therapy of human breast cancer using salicylic acid and methylene blue," Spectrochim. Acta Part A Mol. Biomol. Spectrosc., **184**, 198–203 (2017).

[38] P. Palasuberniam, X. Yang, D. Kraus, P. Jones, K. A. Myers, and B. Chen, "ABCG2 transporter inhibitor restores the sensitivity of triple negative breast cancer cells to aminolevulinic acid-mediated photodynamic therapy," Sci. Rep., **5,** 13298 (2015).

[39] M. Mastrangelopoulou et al., "Predictive biomarkers for <scp>5-ALA-PDT</scp> can lead to personalized treatments and overcome tumor-specific resistances," Cancer Rep., **5**, e1278 (2020).

[40] V. G. Ziegler, J. Knaup, D. Stahl, B. Krammer, and K. Plaetzer, "Fluorescence detection and depletion of T47D breast cancer cells from human mononuclear cell-enriched blood preparations by photodynamic treatment: Basic in vitro experiments towards the removal of circulating tumor cells," Lasers Surg. Med., **43**, 548–556 (2011).

[41] D. L. Holliday and V. Speirs, "Choosing the right cell line for breast cancer research," Breast Cancer Res., **13**, 215 (2011).

[42] L. Rasmussen, Z. Foulks, C. Burton, and H. Shi, "Establishing pteridine metabolism in a progressive isogenic breast cancer cell model," Metabolomics, **18,** 2 (2022).

[43] Y. Qu et al., "Evaluation of MCF10A as a Reliable Model for Normal Human Mammary Epithelial Cells," PLoS One, **10**, e0131285 (2015).

[44] P. Kumar, A. Nagarajan, and P. D. Uchil, "Analysis of Cell Viability by the MTT Assay," Cold Spring Harb. Protoc., 2018, pdb.prot095505 (2018).

[45] A. V. B. Pintor, L. D. Queiroz, R. Barcelos, L. S. G. Primo, L. C. Maia, and G. G. Alves, "MTT versus other cell viability assays to evaluate the biocompatibility of root canal filling materials: a systematic review," Int. Endod. J., **53**, 1348–1373 (2020).

[46] S. Kwiatkowski et al., "Photodynamic therapy – mechanisms, photosensitizers and combinations," Biomed. Pharmacother., **106**, 1098–1107 (2018).

[47] A. F. Dos Santos *et al.*, "Distinct photo-oxidation-induced cell death pathways lead to selective killing of human breast cancer cells," Cell Death Dis., **11**,1070 (2020).

[48] S. Lee and C. A. Schmitt, "Chemotherapy response and resistance," Curr. Opin. Genet. Dev., **13**, 90–96 (2003).

[49] O. Bozkulak, R. F. Yamaci, O. Tabakoglu, and M. Gulsoy, "Photo-toxic effects of 809-nm diode laser and indocyanine green on MDA-MB231 breast cancer cells," Photodiagnosis Photodyn. Ther., **6**, 117–121 (2009).

[50] I. S. Cogno, N. B. R. Vittar, M. J. Lamberti, and V. A. Rivarola, "Optimization of photodynamic therapy response by survivin gene knockdown in human metastatic breast cancer T47D cells," J. Photochem. Photobiol. B Biol., **104**, 434–443 (2011).

[51] T.-M. Don, K.-Y. Lu, L.-J. Lin, C.-H. Hsu, J.-Y. Wu, and F.-L. Mi, "Temperature/pH/Enzyme Triple-Responsive Cationic Protein/PAA- b -PNIPAAm Nanogels for Controlled Anticancer Drug and

Photosensitizer Delivery against Multidrug Resistant Breast Cancer Cells," Mol. Pharm., **14**, 4648–4660 (2017).

[52] P. A. Macêdo-Sales et al., "Coinfection of domestic felines by distinct Sporothrix brasiliensis in the Brazilian sporotrichosis hyperendemic area," Fungal Genet. Biol., **140**, 103397 (2020).

[53] J. Duanmu, J. Cheng, J. Xu, C. J. Booth, and Z. Hu, "Effective treatment of chemoresistant breast cancer in vitro and in vivo by a factor VII-targeted photodynamic therapy," Br. J. Cancer, **104**, 1401–1409 (2011).

[54] G. Guney Eskiler, A. Deveci Ozkan, E. Sozen Kucukkara, A. F. Kamanlı, B. Gunoğlu, and M. Z. Yıldız, "Optimization of 5-aminolevulinic acid-based photodynamic therapy protocol for breast cancer cells," Photodiagnosis Photodyn. Ther., **31**, 101854 (2020).

[55] R. Ghoodarzi, V. Changizi, A. R. Montazerabadi, and N. Eyvazzadaeh, "Assessing of integration of ionizing radiation with Radachlorin-PDT on MCF-7 breast cancer cell treatment," Lasers Med. Sci., **31**, 213–219 (2016).

[56] T. K. Horne, H. Abrahamse, and M. J. Cronjé, "Investigating the efficiency of novel metallo-phthalocyanine PDT-induced cell death in MCF-7 breast cancer cells," Photodiagnosis Photodyn. Ther., **9**, 215–224 (2012).

[57] R. Hosseinzadeh, K. Khorsandi, and G. Hosseinzadeh, "Graphene oxide-methylene blue nanocomposite in photodynamic therapy of human breast cancer," J. Biomol. Struct. Dyn., **36**, 2216–2223 (2018).

[58] Z. Hu, B. Rao, S. Chen, and J. Duanmu, "Targeting tissue factor on tumour cells and angiogenic vascular endothelial cells by factor VII-targeted verteporfin photodynamic therapy for breast cancer in vitro and in vivoin mice," BMC Cancer, **10**, 235 (2010).

[59] J. Rodríguez-Romero et al., "Synthesis, chemical–optical characterization and solvent interaction effect of novel fluorene-chromophores with D–A–D structure," Dye. Pigment., **98**, 31–41 (2013)

[60] A. F. Kamanlı, M. Z. Yıldız, E. Özyol, A. Deveci Ozkan, E. Sozen Kucukkara, and G. Guney Eskiler, "Investigation of LED-based photodynamic therapy efficiency on breast cancer cells," Lasers Med. Sci., **36**, 563–569 (2021).

[61] A. Khanal, M.-P. N. Bui, and S. S. Seo, "Microgel-Encapsulated Methylene Blue for the Treatment of Breast Cancer Cells by Photodynamic Therapy," J. Breast Cancer, **17**, 18 (2014).

[62] K. Khorsandi, E. Chamani, G. Hosseinzadeh, and R. Hosseinzadeh, "Comparative study of photodynamic activity of methylene blue in the presence of salicylic acid and curcumin phenolic compounds on human breast cancer," Lasers Med. Sci., **34**, 239–246 (2019).

[63] J. Płonka, M. Latocha, D. Kuśmierz, and A. Zielińska, "Expression of Proapoptotic BAX and TP53 Genes and Antiapoptotic BCL-2 Gene in MCF-7 and T-47D Tumour Cell Cultures of the Mammary Gland After a Photodynamic Therapy with Photolon," Adv. Clin. Exp. Med., **24**, 37–46 (2015).

[64] C. I. M. Santos et al., "Enhanced Photodynamic Therapy Effects of Graphene Quantum Dots Conjugated with Aminoporphyrins," ACS Appl. Nano Mater., **4**, 13079–13089 (2021).

[65] A. Sazgarnia, A. R. Montazerabadi, M. H. Bahreyni-Toosi, A. Ahmadi, and A. Aledavood, "In vitro survival of MCF-7 breast cancer cells following combined treatment with ionizing radiation and mitoxantrone-mediated photodynamic therapy," Photodiagnosis Photodyn. Ther., **10**, 72–78 (2013).

[66] A. Uppal, B. Jain, P. K. Gupta, and K. Das, "Photodynamic Action of Rose Bengal Silica Nanoparticle Complex on Breast and Oral Cancer Cell Lines," Photochem. Photobiol., **87**, 1146–1151 (2011).

[67] H. Wang et al., "Combination of a Novel Photosensitizer DTPP with 650 nm Laser Results in Efficient Apoptosis and Cytoskeleton Collapse in Breast Cancer MCF-7 Cells," Cell Biochem. Biophys., **69**, 549–554 (2014).

[68] H.-P. Yeh, A. C. del Valle, M.-C. Syu, Y. Qian, Y.-C. Chang, and Y.-F. Huang, "A New Photosensitized Oxidation-Responsive Nanoplatform for Controlled Drug Release and Photodynamic Cancer Therapy," ACS Appl. Mater. Interfaces, **10**, 21160–21172 (2018).

[69] A. Y. Sadeghloo, K. Khorsandi, and Z. Kianmehr, "Synergistic effect of photodynamic treatment and doxorubicin on triple negative breast cancer cells," Photochem. Photobiol. Sci., **19**, 1580–1589 (2020).

[70] J. Zhu et al., "Inhibition of breast cancer cell growth by methyl pyropheophenylchlorin photodynamic therapy is mediated though endoplasmic reticulum stress-induced autophagy in vitro and vivo," Cancer Med., **7**, 1908–1920 (2018).

[71] L. Song et al., "O 2 and Ca 2+ Fluxes as Indicators of Apoptosis Induced by Rose Bengal–Mediated Photodynamic Therapy in Human Oral Squamous Carcinoma Cells," Photomed. Laser Surg., **33,** 258–265 (2015).

[72] M. Osuchowski et al., "Photodynamic Therapy-Adjunctive Therapy in the Treatment of Prostate Cancer," Diagnostics, **12**, 1113 (2022).

[73] A. C. Croce, E. Wyroba, and G. Bottiroli, "Distribution and retention of rose bengal and disulphonated aluminium phthalocyanine: A comparative study in unicellular eukaryote," J. Photochem. Photobiol. B Biol., **16**, 318–330 (1992).

[74] C. Soldani et al., "Apoptosis in tumour cells photosensitized with Rose Bengal acetate is induced by multiple organelle photodamage," Histochem. Cell Biol., **128**, 485–495 (2007).

[75] D. P. Valenzeno, J. Trudgen, A. Hutzenbuhler, and M. Milne, "Singlet oxygen involvement in photohemolysis sensitized by merocyanine-540 and rose bengal," Photochem. Photobiol., **46**, 985–990 (1987).

[76] I. E. Kochevar, J. Bouvier, M. Lynch, and L. Chi-Wei, "Influence of dye and protein location on photosensitization of the plasma membrane," Biochim. Biophys. Acta - Biomembr., **1196**, 172–180, (1994).

[77] N. Sugita, Y. Iwase, N. Yumita, T. Ikeda, and S.-I. Umemura, "Sonodynamically induced cell damage using rose bengal derivative.," Anticancer Res., **30**, 3361–6 (2010).

1. Introduction

Breast cancer stands as one of the most critical global health challenges and remains a leading cause of cancer-related deaths in women across various regions [1-2]. According to the Global Cancer Observatory (GLOBOCAN, the interactive website of the International Agency for Cancer Research of the World Health Organization), breast cancer was reported as the most commonly diagnosed cancer worldwide, with 2.26 million cases reported in 2020 [3]. To combat this disease, diverse techniques are employed, including surgery [4], radiation therapy [4-5], chemotherapy [4], hormonal therapy [4,6], and immunotherapy [7]. However, these approaches are often aggressive and heavily rely on early-stage diagnosis for optimal efficacy [8-9]. This dependence can prove challenging, particularly when conventional therapies are not viable, such as in the case of triple-negative breast cancer, where targetable proteins like the estrogen receptor are absent, and HER2 amplification is lacking. Moreover, the emergence of treatment resistance is a common occurrence in endocrine therapy, anti-HER2 therapy, and chemotherapy [4, 10], requiring exploration of alternative treatments. Among the alternatives, photodynamic therapy (PDT) emerges as a promising option, particularly for breast cancer, offering advantages over conventional therapies such as no ionizing radiation is used, is localized, minimally invasive, and cost-effective [11-13]. The procedure involves the application of a photosensitizer (PS) activated by light of a specific wavelength. In the presence of oxygen, this process generates reactive oxygen species and/or singlet molecular oxygen, triggering the activation of biological mechanisms leading to cell death [14-15].

While visible light has a limited penetration depth (0.5 to 2.5 mm) into biological tissues [16], it holds significant potential for various clinical applications in PDT. This includes treating superficial infections, cancers, and injuries [17]. Additionally, it can aid as an auxiliary treatment during surgery, particularly in

cases where complete resection is not achievable [18]. Moreover, advancements in light delivery technology are facilitating the utilization of optical fibers to penetrate deeper into tissue [19-20].

The high photochemical reactivity of PS, leading to the generation of reactive oxygen species or singlet oxygen, is often the crucial factor of success in PDT [21-22]. However, other crucial factors come into play, such as the PS's ability to be absorbed by cells. The nature and electrical charge of each PS influence its capacity to traverse cell membranes and localize within intracellular sites [1]. The intracellular localization of a PS is intimately linked to its mode of action, potentially influencing both primary and secondary reactive oxygen species production and thereby dictating different cellular outcomes [2-3]. Oliveira et al. suggest that subcellular localization may be even more critical than photochemical reactivity for overall cell destruction [8].

Hydrophilic PS tend to preferentially target charged substructures like mitochondria or lysosomes [9,11]. On the other hand, lipophilic anionic PS primarily reside in cell plasma membranes and subcellular organelles [12]. Certain PS, such as methylene blue (MB), may localize in various subcellular sites such as mitochondria, lysosomes, and membranes [13], while others, like anionic substances, struggle to penetrate cells effectively. For instance, rose Bengal (RB) exhibits low lipid solubility, impairing its ability to traverse biological membranes [14], often necessitating the use of carriers or adjuvants to facilitate cellular entry [15,23-24]. Several PS have been extensively studied in PDT for cancer treatment, particularly porphyrin derivatives, which have been explored in bladder, lung, cervical, endobronchial, basal cell, esophageal, and breast cancers [25-26]. However, non-porphyrin PS, such as MB and RB, are rarely utilized for PDT in breast cancer treatment.

In this study, we selected two non-porphyrin PS from different chemical families: RB and MB. RB is an anionic dye belonging to the xanthene family, soluble in water, and clinically employed as a diagnostic agent for ophthalmological disorders and liver function [27]. Despite its poor penetration of cell membranes, RB stands out as an excellent PS due to its coefficient of singlet oxygen generation (0.76) [27-28]. On the other hand, MB is a dye from the phenothiazine family, widely utilized in clinical settings for staining microorganisms, as an indicator in various surgical techniques, for detecting intestinal, enterovesical, and bronchopleural fistulas, and for treating methemoglobin-induced encephalopathy, among other applications [29]. The absorption spectrum of MB depends on its atomic structure, which also allows for dimer formation. The monomeric and dimeric forms exhibit distinct absorption spectra, with the monomeric form showing an absorption peak at 664 nm and the dimeric form at 590 nm. The permeation of MB through membranes is attributed to the diffusion of MB monomers [13].

On the other hand, among the breast cancer cell lines studied *in vitro*, MCF7 [30-36] and ductal adenocarcinoma MDA-MB-231 are the most extensively researched, with only a few reports on non-porphyrinic PDT studies, including hypericin or MB [32,34-37]. For other types of breast cancer cells, such as T47D cells, there is almost no literature on PDT studies with non-porphyrin PS, with reports limited to PDT with porphyrin PS [38-40]. Here, we used a breast cell that has hardly been studied in PDT, such as T47D. This is an epithelial cell line of the mammary gland that causes ductal carcinoma, positive for estrogen and progesterone [41], and compare their ability to capture the PS and their response to PDT with cancer cells of epithelial origin from metastatic breast adenocarcinoma MDA-MB231. MDA-MB231 is a triple-negative cell line that is highly aggressive, invasive and poorly differentiated, lacking expression of the estrogen receptor, progesterone receptor and HER2 receptor [41]. Finally, we utilized the human mammary epithelial cell line, MCF10A, an immortalized cell line dependent on adhesion for survival widely employed in vitro studies. This model serves to investigate normal mammary cell function and transformation [42]. It is the most widely used non-cancerous breast cell line for in vitro assays. However, it exhibits a unique, differentiated phenotype in 3D culture that may be absent or rare in normal human breast tissue[43]. This cell has been useful to compare cancer and non-cancer susceptibility to PDT.

2. Materials and methods

2.1. Cell cultures

Three breast cell lines were used. MDA-MB-231 (ATCC HTB-26™) was maintained in Leibovitz medium (L-15; Sigma-Aldrich) with heat-inactivated fetal bovine serum (FBS) at 10% (Biowest). T47D cell line (ATCC HTB- 133™) was maintained in RPMI 1640 (Sigma-Aldrich) with 10% FBS, insulin (0.2 U/ml; Sigma-

Aldrich). The MCF10A cell line (ATCC CRL-10317™) was maintained in Ham's F12 (Biowest) supplemented with epidermal growth factor (100 µg/ml), hydrocortisone (1 mg/ml Sigma-Aldrich), 10% horse serum (Biowest), *Vibrio cholerae* cholera toxin (1 mg/ml) (Sigma-Aldrich), and insulin (0.1%) (Sigma-Aldrich).

Cell cultures were maintained in a humidified incubator (Hinotek, China) at 37° C in a 5% CO_2 atmosphere in a T-25 culture box (Corning). For subsequent experiments, cells were detached by trypsinization (trypsin 0.025%, EDTA 0.01%; Gibco) and washed with phosphate-buffered saline (PBS). All culture media were supplemented with 100 U/ml penicillin and 100 µg/ml streptomycin (Sigma-Aldrich).

2.2. PS and light source

We prepared a stock solution of each PS, MB from Omnichem, Mexico, and RB from Meyer, Mexico, at concentrations of 200 µM and 100 µM, respectively, in 1X PBS. To ensure sterility, we filtered this solution using syringe filters (0.22 µm, GVS Life Sciences, USA). Subsequently, we generated a working solution according to the concentrations determined in the test for use in PDT treatments. Two LED-based light devices were employed for irradiations. These devices feature an array of 12 LEDs, a heat-dissipating surface, and a support for 96-well microplates. The red-light device (600-650 nm) activated MB, with a peak emission at 630 nm, while the green-light device (490-540 nm) activated RB with a peak emission at 500 nm. The power of each LED was measured with a power meter (Thorlabs pm100d) and was determined to average 33.6 mW.

2.3. Intracellular quantification of the PS

The absorption spectrum of the PS was measured with a spectrophotometer (Synergy text trademark 4, VT, EE. UU) using 100 µM of MB (Omnichem, Mexico) and 50 µM of RB (Meyer, Mexico), both dissolved in 1X PBS. To quantify intracellular PS, 1.5 x 10^4 cells were inoculated into each microplate well. After 24 h of incubation at 37°C, the samples were washed with 100 µl of PBS, (100 µl) a solution of culture media containing 20 µM MB or 7 µM RB was added and incubated again for 2 h. After this time, the supernatant was removed, and each well was washed twice with PBS. A change in osmotic pressure was used to lyse the cells by adding 100 µl of injectable water (PiSA, México), to finally collect the absorption spectrum in the 450-700 nm range was obtained using an ELISA reader (Synergy, BioTek).

2.4. PDT application

For each cell line, 1.5 x 10^4 cells were inoculated into each well of a 96-well microtiter plate and incubated for 24 h in their respective culture medium. They were washed with PBS and incubated with the PS solution for 1 h at 37°C. Two PS were used: MB at 5, 10, and 20 µM in PBS, activated with 10 J/cm^2 of red light (MB belongs to the phenothiazinium family and absorbs at 666 nm with maximum molar absorption coefficient ε_{max} ~ 82,000 /M*cm [26]. RB at 3, 5, and 7 µM in PBS, activated with 8 J/cm^2 of green light. RB is a water soluble xanthene sensitizer that absorbs at 549 nm with ε_{max} ~ 100,000/M*cm [26]. The cells were washed twice with PBS to remove any PS that was not taken up by the cells. Then, 100 µl of PBS was added to each well for subsequent irradiation. Immediately after irradiation, the microtiter plates were incubated with the appropriate culture media for 24 h at 37°C in a 5% CO_2 atmosphere. All treatments were performed in triplicate (n = 3) with the corresponding controls: cells exposed to PS only (dark toxicity control), cells only exposed to light (phototoxicity control), and cells without any treatment (control cells), not exposed to PS or light.

2.5. Evaluation of cell viability

The MTT assay (Sigma-Aldrich)[44], [45] was used to determine cell viability 24 h after each cell line was subjected to PDT. The resulting formazan was dissolved with dimethyl sulfoxide (DMSO) (Sigma-Aldrich), and its concentration was determined by optical density measurement at 570 nm. Cell viability was calculated using the following equation:

$$\% \text{ viability} = (\text{O.D. treated cells} / \text{O.D. control cells}) \times 100$$

where O.D. is the optical density of cells.

2.6. Evaluation of morphological changes in the treated cells

The morphologic effects of PDT in cell lines were evaluated using photographs taken 24 h after application of MB-PDT and RB-PDT using an inverted microscope at 20X for MDA-MB-231 and T47D cells and 10X for MCF 10A cells.

2.7. Statistical analysis

Statistical analysis was performed on the viability assay results using one-way ANOVA analysis with Tukey multiple comparison test. A value of $p < 0.05$ was considered statistically significant.

3. Results

3.1. Determination of PS in cell cultures

The absorption spectrum confirmed the presence of MB inside the three cell lines that were incubated with this PS. The peak absorption was observed at 670 nm, which was not present in the corresponding controls (**Figure 1**). Specifically, the non-cancerous breast cell line MCF10A and the cancer cell line T47D exhibited higher intracellular levels of MB compared to the cancer cell line MDA-MB-231 (**Figure 1a**). Conversely, in cells incubated with RB (**Figure 1b**), no absorbance peak was evident at 550 nm, precluding the observation of RB's intracellular presence.

3.2. PDT efficiency

The results obtained in MDA-MB-231 and T47D cell lines using PDT with MB and RB showed that cell viability decreased with increasing concentration of FS and energy density (**Figure 2**). MDA-MB-231 adenocarcinoma cells were the most sensitive to PDT with both PS, showing viabilities less than 40% with MB PDT and less than 50% with RB PDT. The T47D breast cancer cells reduced their viability by almost 50% in both cases. Finally, MCF10A non-cancerous breast cells showed an interesting behavior, as there was no significant inhibition response with MB-PDT, although there was with RB-PDT (**Figure 2**).

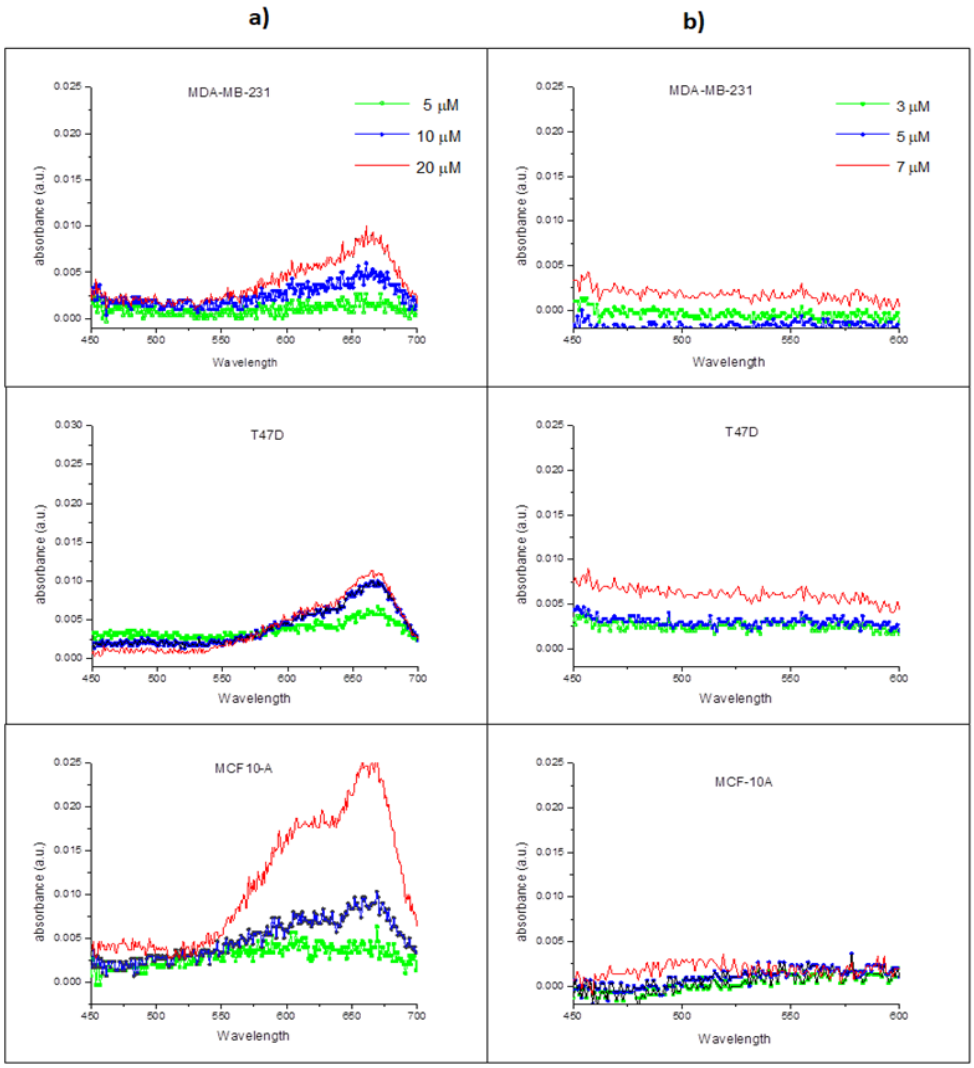

Figure 1. Intracellular presence of MB (a) and RB (b) in three breast line cells after 1 h of incubation (values were obtained by subtracting the control value from each measured absorbance).

3.3 Morphological changes caused by PDT

The typical phenotypes of the MDA-MB-231, T47D, and MCF10A cell lines, show spindle cells, some more elongated than others, which is characteristic of routine cell cultures. The control cell cultures, without any treatment, were observed to be homogeneous in the nuclear-cytoplasmic relationship in terms of size, arrangement and spacing. One or two nucleoli and fine granulations in the cytoplasm were observed. There were very few contracted cells, possibly dead by apoptosis due to natural turnover (**Figure 3, column 1**). In contrast, PDT-treated cells show a decrease in confluence and contraction of the cell membrane was observed, their area decreased, they lost adherence and became rounded. Rounded cells predominated in the two cancer cell lines, where the cytoplasm was significantly reduced (**Figure 3: b and c, column 4**). Cancer cells shows high mortality rate, since most of them were pyknotic (i.e. shrunken cytoplasm and a condensed, darkly stained nucleus), in contrast to what was observed in the non-cancerous cell line (MCF-10A), which maintained a morphology similar to that of the control. Also, cells treated with RB-PDT showed apparent cytopathic damage, similar to that described above, in both breast cancer cell lines and non-cancerous cells (**Figure 3: d-f, column 4**).

a) **b)**

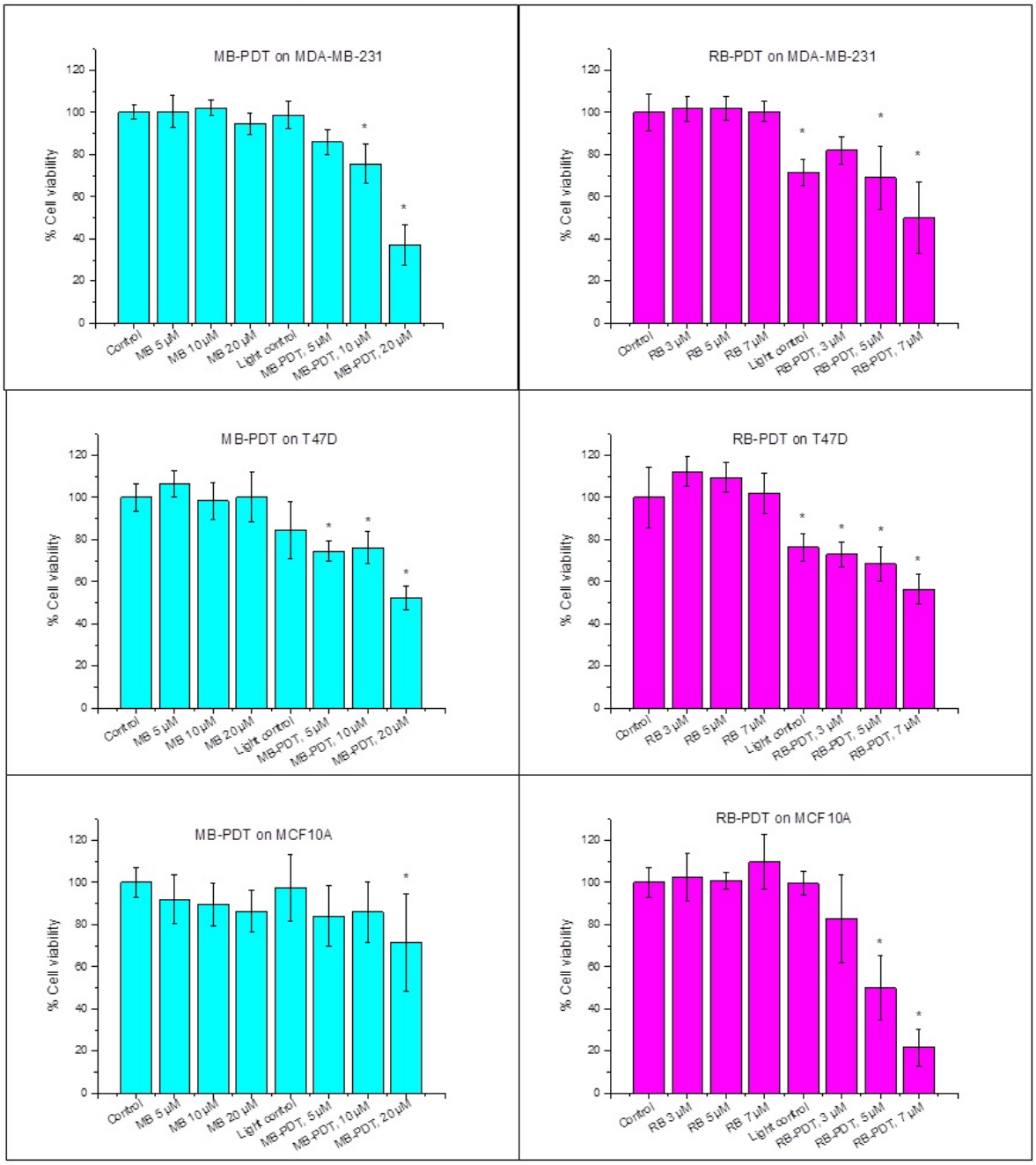

Figure 2. Cell viability values of the cell lines with a) MB-PDT and, b) RB-PDT MDA-MB-231. Data are expressed as the mean of 3 independent experiments performed in triplicate * $p < 0.05$.

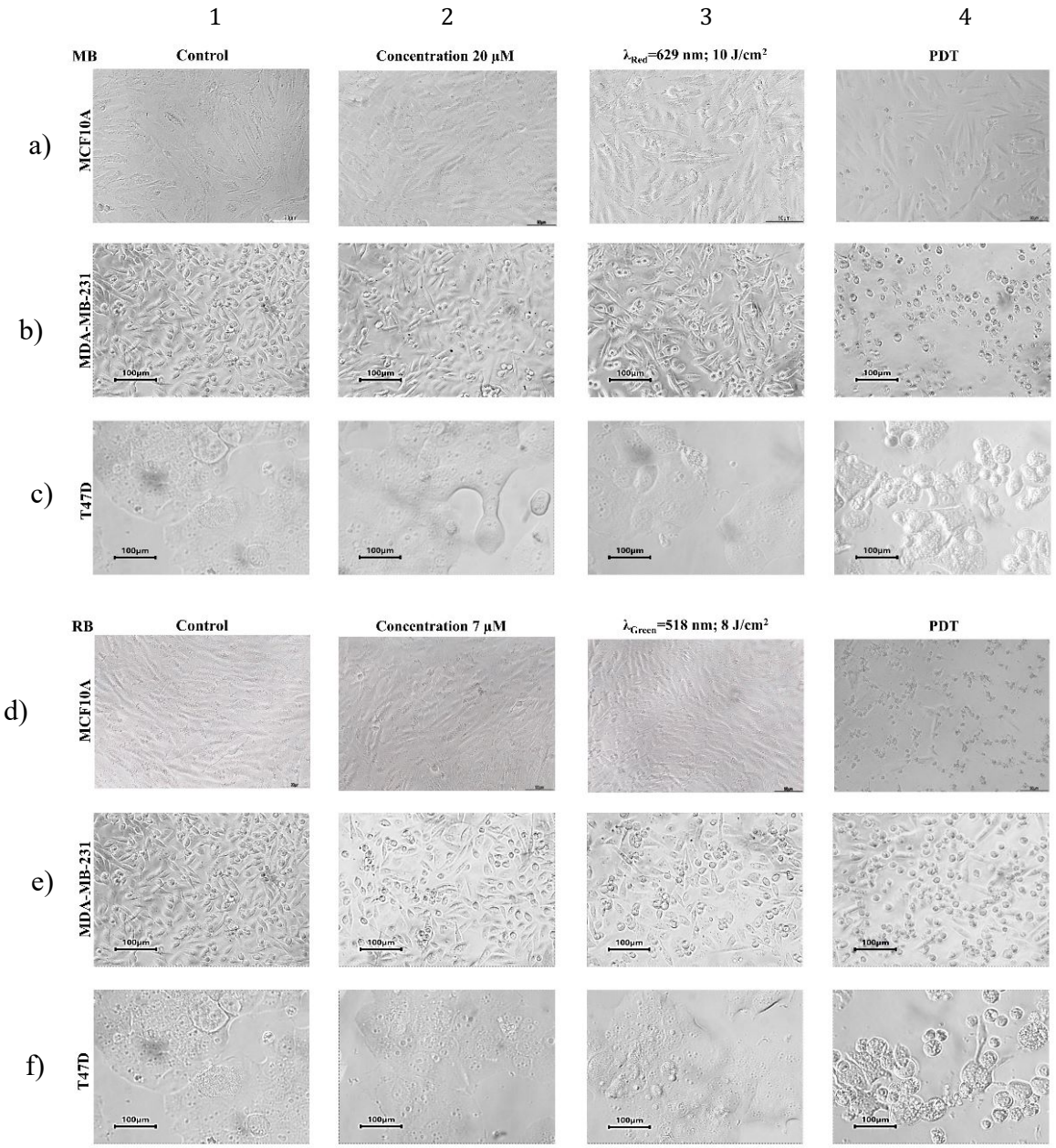

Figure 3. Representative images of the effect of MB-PDT and RB-PDT with their respective controls on cancerous and non-cancerous cell lines. Images were taken 24 hours after the PDT application and observed with an inverted light microscope (Leica) at 20X for the MCF10A and MDA-MB-231 cell lines and 10X for the T47D cell line.

The light controls also showed some important differences from the control, especially the green light (8 J/cm^2). A cytopathic effect of light was observed, characterized by an increase in the number of rounded and lysing cells, see **Figure 3e, column 3**. In contrast, the control cells for the FS did not show significant morphological changes compared to the untreated control in any of the 3 cell lines evaluated (**Figure 3: column 2**).

4. Discussion

The results of this study provide important contributions to the understanding of PS effect in cell cultures, the effectiveness of PDT, and the resulting morphological changes in cells. In breast cancer research, PDT

has primarily focused on cell lines like MCF7 and MDA-MB-231, with a predominant use of PS from the porphyrin family or their derivatives (**Table 1**). However, there is a lack of literature reports regarding RB-PDT in MB-MDA-231 cells and RB-PDT and MB-PDT in T47D luminal cancer cells. Comparative studies of PDT between cancer cells and non-cancerous MCF-10A cells are also limited. Palasuberniam et al. [38] has explored ALA in various breast cell lines and dos Santos et al. [36], reported increased sensitivity of MB-MDA-231 cancer cells compared to MCF-10A cells using MB as the PS. There are currently no reports on RB-PDT in MCF-10A cells. Previous studies have suggested that cancer cells exhibit higher sensitivity to PDT compared to normal cells [11,37-38]. This increased sensitivity in cancer cells may be attributed to the preferential accumulation of PS within cancer cells, facilitated by the higher presence of low-density lipoproteins in their cell membranes [46].

The findings of our study support the selective nature of MB-PDT towards cancer cells. When applying a dose of 20 μM and 10 J/cm^2, a high survival rate of 80% was observed in MCF-10A cells (normal cells), while considerably lower survival rates of 38% and 52% were observed in MB-MDA-231 and T47D cells (cancer cells), respectively. These results indicate that normal cells exhibit a higher tolerance to MB-PDT compared to cancer cells at the same dose. In contrast, the sensitivity of normal cells to RB-PDT was found to be equal to (at a dose of 3 μM and 8 J/cm^2) or even greater than (at doses of 5 or 7 μM and 8 J/cm^2) that of cancer cells. This suggests that RB-PDT may exert similar or stronger cytotoxic effects on normal cells compared to cancer cells under the evaluated conditions.

The analysis of the absorption spectrum provided strong evidence for the successful uptake of MB by all three cell lines, as indicated by the presence of a distinct absorption peak at 670 nm. Notably, the non-cancerous breast cell line MCF10A and the cancer cell line T47D exhibited higher levels of intracellular MB compared to the cancer cell line MDA-MB-231. This observation suggests variations in the uptake and accumulation of MB among different cell types.

While the exact reasons for the preferential uptake of MB are not fully understood, it is plausible to consider the involvement of specific membrane receptors. For instance Qu et al. [43] reported that MCF10A cells can exhibit a basal-like phenotype and simultaneously expressing luminal markers, such as cytokeratin markers (CK5 or CK17). These markers play a role in apoptosis, protein synthesis modulation, epithelial polarity, and interactions with associated proteins. It is possible that these markers contribute to the interaction of MB with the cell membrane and its subsequent uptake, as observed in T47D cells, in contrast to basal-like cells like MDA-MB-231 that typically lack these markers. Additionally, Dos Santos et al. [47] reported that the efficiency and selectivity of MB-PDT depend on polyunsaturated fatty acid-enriched membranes and the better ability to cope with photooxidative damage exhibited by non-tumorigenic cells. MDA-MB-231 cells were found to be more susceptible to ferroptosis than MCF10A cells due to their inability to cope with lipid peroxidation. However, it is important to note that the intracellular concentration of the PS does not necessarily correlate with the obtained effect in the PDT process. Despite the higher concentration of MB found in T47D tumor cell lysates, the inhibitory effect was slightly higher in MDA-MB-231 cells. This discrepancy may be attributed to complex signaling networks that influence apoptotic or survival processes [48].

TABLE 1.PS commonly used in PDT for breast cancer cells.

REFERENCE	CELL LINE	PS
[49]	MDA-MB-231	Indocyanine green
[50]	T47D	Methyl Aminolevulinate (MAL)
[51]	MCF-7 and MCF-7/ADR	RB-loaded nanogels
[36]	MDA-MB-231 and MCF-10A	MB
[52]	MDA-MB-231 and MCF-7	MB

[53]	MCF-7/MDR	Factor VII-targeted Sn (IV) chlorin e6
[54]	MCF-7 and MDA-MB-231	Aminolevulinic Acid (ALA)
[30]	MCF-7 and MDA-MB-231	Hypericin
[55]	MCF-7	Radachlorin
[56]	MCF-7	Metallo-phthalocyanine
[57]	MDA-MB-231	MB-graphene oxide nano-sheets
[37]	MDA-MB-231	MB y MB with salicylic acid
[58]	CHO-K1	Verteporfin
[59]	MDA-MB-468	Nanoparticles and MB
[60]	MDA-MB-231 and MCF-7	ALA
[61]	MCF-7	MB in microgel
[62]	MDA-MB-231	MB-curcumin and MB-salicylic acid complexes
[15]	HCC70	PLGA/RB colloidal particles
[39]	MCF7, MDA-MB-231, and T47D	5-ALA
[31]	MCF-7	Indocyanine green
[34]	MCF-7	Sulfur-doped graphene and MB
[33]	MCF-7	RB
[38]	T47D, MCF-10A, SkBr3, Hs-578T, MDA-MB-231, MDA-MB-453 and MDA-MB-361	ALA
[63]	T47D and MCF-7	Photolon® – a chlorin e6 (Ce6) and polyvinylpyrrolidone (PVP)
[64]	T47D	Graphene quantum dots conjugated with amino porphyrins
[65]	MCF-7	Mitoxantrone
[35]	MDA-MB-231 and MCF7	Hypericin PDT–tamoxifen hybrid therapy
[66]	MCF-7	RB-silica nanoparticle complex
[67]	MCF-7	DTPP
[67]	MCF-7	RB-grafted biodegradable microcapsules
[68]	MCF-7	RB-loaded polymeric MNCs
[69]	MDA-MB-231	Doxorubicin and MB
[40]	T47D	ALA

[70]	MDA-MB-231	Methyl pyropheophenylchlorin

RB has been used in the elimination of some types of cancer cell lines, such as oral squamous cell carcinoma [71] or prostate cancer cells [72]. RB is an anionic, hydrophilic PS that does not readily penetrate eukaryotic cells due to its high lipid content membranes. The uptake of RB into eukaryotic cells can be enhanced when it is accompanied by lipoproteins [73] or when an acetate group is added, which increases its hydrophobicity [74]. If this is not done, the RB disodium salt may remain bound to the cell membrane [22], [27,40]. Valenzeno et al. [75] reported the localization of RB at the membrane interface, as they did not detect the presence of the PS in the supernatant. This likely explains why no distinct peak at 550 nm was observed in the cells exposed to RB in our study, indicating that the intracellular presence of RB could not be confirmed in any of the three cell lines examined.

The mechanism underlying RB-induced cell death in PDT may involve singlet oxygen interacting at the membrane level [28]. Kochevar et al (1994) suggest that RB selectively binds to membrane sites and induces plasma membrane damage upon illumination at 514 nm. They found that RB induces a change in membrane potential in the absence of light. They also confirmed that the highest incident dose, 20 J/cm2, does not affect the membrane potential when photosensitizing dyes are not present [76]. RB's excellent singlet oxygen quantum yield, which is close to 100% [77], and its interaction with the membrane potential may be the reason for its effectiveness as a PS. Given that it has been reported that singlet oxygen activity can also lead to extracellular activation of the FAS/TNF receptor, triggering a signaling cascade that induces apoptosis [3,8,22]. Therefore, it is plausible that RB-PDT in our study induces cell death through membrane-level interactions. Understanding the uptake and intracellular localization of RB, as well as elucidating the specific mechanism of RB-induced cell death, is crucial for optimizing its therapeutic potential in PDT. Further research is needed to explore the underlying molecular processes and signaling pathways involved in RB-PDT, which will contribute to enhancing its efficacy and broadening its applications in cancer treatment.

These findings highlight the intricate interplay between PS uptake, intracellular concentration, and the downstream effects observed during PDT. Further research is warranted to elucidate the precise mechanisms underlying the variations in MB uptake among different cell types and to unravel the signaling networks that govern the differential response to PDT. As well as pertinent studies for *in vivo* applications. Such knowledge can contribute to the development of more targeted and effective PDT in the future.

5. Conclusions

This study demonstrates the successful uptake of MB by all cell lines, as well as the fact that the internalized concentration of MB was not proportional to the inhibition effect observed in the different cell lines. Just as no intracellular RB was found. This study presents, to the best of our knowledge, the first evidence of the inhibitory effect of PDT using RB as a PS on MDA-MB-231, T47D and MCF10A cells. Which resulted in efficacy in inhibiting both cancerous and non-cancerous cells. Additionally, the study reports, for the first time, the effect of PDT with MB as a PS to inhibit the T47D cell line. The MDA-MB-231 cell line exhibited the highest sensitivity to PDT, while the non-cancerous MCF10A cells showed some resistance to MB-PDT. Morphological changes, indicative of cell death, were observed in all cells studied, especially in cancer cells and at the highest doses. It is noteworthy that non-cancerous MCF10A cells showed notable changes only with the highest dose of RB-PDT. Finally, these findings highlight the potential of MB and RB as effective PS in PDT and suggest the importance of considering cell line-specific responses and characteristics in optimizing PDT efficacy and selectivity.

